

Chapter 1

NMR - Basic Theory

Nuclear Magnetic Resonance (NMR) spectroscopy is one of the most powerful analytical tools in modern science. Basic research regarding phase transition, quantum rotational tunneling, molecular dynamics and structure analysis has been carried out using this technique. Structural investigations by NMR provide a valuable supplement to X-ray spectroscopy in structure analysis. NMR is indeed an indispensable tool for a modern scientist. The application of NMR to modern day science has extended from the study of chemical dynamics to functional group analysis, medical diagnosis, bonding connectivity and orientation, molecular conformations and even to 3D imaging to resolutions of the order 1 mm. This technique can give information about non-crystalline solids also.

In this introductory chapter, a brief outline of the basic theory of the magnetic resonance phenomenon and topics relevant to the present work are given. Measurement techniques of second moment and spin lattice relaxation times with special emphasis to different magnetization recovery profiles for different pulse sequences used in the present investigations are also discussed in this chapter.

1.1 Nuclear Spins in a Static Magnetic field

Spin, the intrinsic quantum mechanical property of many fundamental particles or combinations of particles, is described by equations treating angular momentum. Each nucleus (having nuclear spin \vec{I} with angular momentum \vec{J} is associated with a magnetic moment $\vec{\mu}$, is given by

$$\vec{\mu} = \gamma \vec{J}; \quad \vec{J} = \hbar \vec{I}, \quad (1.1)$$

where γ is the gyromagnetic ratio, characteristic of the given nucleus. The z component of a nuclear spin I has a (2I +1) fold degeneracy, which can be lifted with an external static magnetic field. When a static magnetic field H_0 is applied along the z direction, the energy of the nuclear spin can be written as

$$H = -\vec{\mu} \cdot \vec{H} = -\gamma \hbar I_z E_m = -m \gamma \hbar H_0, \quad (1.2)$$

where m is the magnetic quantum number and has (2I+1) values from -I, -I +1,I-1, I. For spin quantum number I = 1/2, the allowed energy eigenvalues are $\pm \gamma \hbar H_0/2$ corresponding to $m = \pm 1/2$. The energy difference between the nuclear states for I = 1/2 is

$$E_{-1/2} - E_{+1/2} = \Delta E = \gamma \hbar H_o = \hbar \omega_o, \quad (1.3)$$

where $\omega_o = \gamma H_o$ is the Larmor frequency.

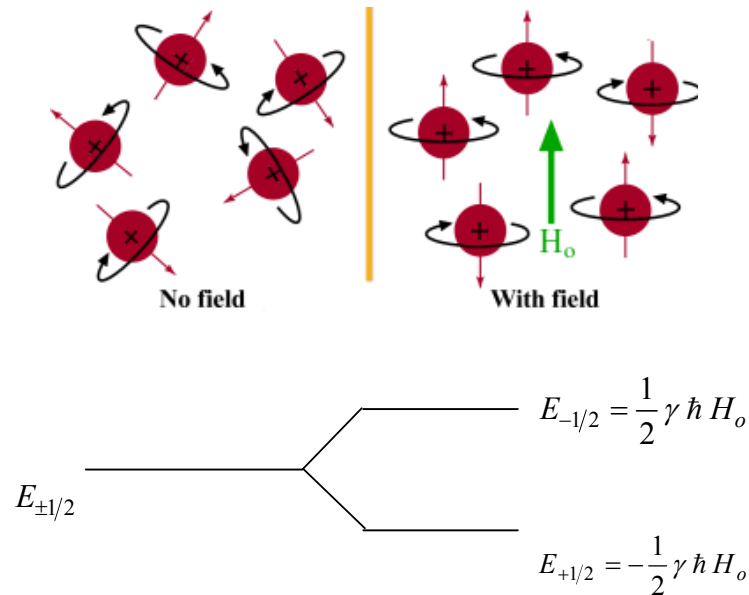


Figure 1.1 Schematic representation of alignment of atomic nuclei and energy levels for a nuclear spin (1/2) in the presence of an external magnetic field.

Figure 1.1 shows the distribution of atomic nuclei in the presence of an external magnetic field and its energy level diagram for a nucleus with spin $I = 1/2$. The energy difference between two successive magnetic field split levels, $\Delta E = \gamma \hbar H_o$, is of the order of radio frequency (10^6 Hz). A typical NMR experiment involves either the detection of the energy required to excite the spins to higher energy level (Wide-line) or the exciting the spins to the higher state and subsequent detection of the energy given out by the spins. Hence, the typical energy involved in NMR experiment is of the order of a nano-electron volt.

In a NMR experiment, the nuclear spin system is irradiated by a radio frequency (RF) field (applied in the xy-plane), the frequency of which can be changed appropriately. When the resonance condition is satisfied, that is when $\omega_o = \gamma H_o$, nuclear spins in the lower energy state absorb energy and go to the higher energy state. If the transition causes a detectable change in the experiment, the fact that a resonance has occurred can

be ascertained and the measurement of ΔE is reduced to a measurement of frequency. Any resonance experiment involves two steps: (1) ‘induce’ or ‘drive’ the resonance, (2) detect its occurrence. Details of detection are discussed later.

Once the nuclear spin system absorbs energy, it relaxes back to its initial energy state. To see how the nuclear spin system relaxes back, consider a macroscopic system, where N nuclear spins of spin $I = 1/2$ kept in a magnetic field H_0 . Out of the N nuclei, N_+ nuclei are in the state with $m = 1/2$ and N_- nuclei are in the state with $m = -1/2$ at thermal equilibrium. With the application of a radio frequency field perpendicular to the static magnetic field H_0 at ‘Larmor frequency’ ω_0 , ‘resonance’ occurs, and the population changes, which can be represented by an equation

$$\frac{dN_+}{dt} = N_- W_{- \rightarrow +} + N_+ W_{+ \rightarrow -} . \quad (1.4)$$

Equation 1.4 is the rate of change of population of $m = +1/2$ state. $W_{+ \rightarrow -}$ denotes the probability per second of inducing the transition of a spin with $m = +1/2$ to a state with $m = -1/2$ and $W_{- \rightarrow +}$ denotes the probability for the reverse process. From the time-dependent perturbation theory, the probability per second $P_{a \rightarrow b}$ that a time dependent interaction $V(t)$ induces a transition from a state (a) with energy E_a to a state (b) with energy E_b is written according to Fermi’s Golden Rule as [1]

$$P_{a \rightarrow b} = 2\pi \left| \langle b | V(t) | a \rangle \right|^2 \delta(E_a - E_b - \hbar\omega) / \hbar . \quad (1.5)$$

Since

$$\left| \langle b | V(t) | a \rangle \right|^2 = \left| \langle a | V(t) | b \rangle \right|^2$$

it follows that $W_{+ \rightarrow -} = W_{- \rightarrow +} = W$. Using the variables $n = N_+ - N_-$ (the difference in the population of two levels), $N = N_+ + N_-$ and we can rewrite the above equation as

$$\frac{dn}{dt} = -2W n . \quad (1.6)$$

The rate of absorption of energy by the spin system can be written as

$$\frac{dE}{dt} = N_+ W \hbar \omega - N_- W \hbar \omega = n W \hbar \omega . \quad (1.7)$$

From Eqn. 1.7 it can be seen that ‘n’ has to be non-zero for absorption of energy by the spin system [2]. This means that there must be a population difference between the energy states for a net absorption of energy. From the solution of equation 1.6, that is

$$n = n_0 e^{-2Wt},$$

where n_0 is the value of ‘n’ at $t = 0$, it is seen that the population difference will eventually vanish and hence resonance also disappears under the action of induced radio frequency transitions. The nuclear spins, which are in the excited state, can relax back to the thermal equilibrium state provided there is something else (a reservoir) that can accept energy from the spins. This reservoir is generally known as the “lattice”. The spin system can continue giving energy to the “lattice” until the relative populations N_-/N_+ correspond to the temperature T of the “lattice”. In fact, a characteristic time that can be associated with the thermal equilibration process between the spin system and the “lattice” is known as the “Spin-Lattice Relaxation (SLR) time” denoted as T_1 . The “spin-lattice relaxation” can also be understood as the time required to magnetize an unmagnetized sample. The rate equation for the population difference ‘n’ in the presence of radio frequency field and thermal processes can be written as

$$\frac{dn}{dt} = -2nW + (n_0 - n)/T_1. \quad (1.8)$$

In the steady state, Eqn 1.8 implies that

$$n = n_0 / (1 + 2W T_1). \quad (1.9)$$

From Eqn. 1.9, it follows that the absorption of energy from the radio frequency field does not disturb the thermal equilibrium population values as long as $2WT_1 \ll 1$. The power absorbed by the nuclei can be increased by increasing the amplitude of the radio frequency field, as long as the above-mentioned condition is satisfied. Once W is large enough so that $W \sim 1/2 T_1$, the power absorbed levels off despite an increase in W . This effect is called ‘saturation’. It is possible to measure T_1 by observing the saturation effect.

1.2 The Classical Picture of Motion

The equation of motion for the nuclear magnetic moment $\vec{\mu}$ is

$$\frac{d\vec{J}}{dt} = \vec{\mu} \times \vec{H} \quad (1.10)$$

or equivalently

$$\frac{d\vec{\mu}}{dt} = \vec{\mu} \times (\gamma \vec{H}) \quad (1.11)$$

The rotating frame of reference

Equation 1.10 can be understood by invoking the concept of rotating coordinates. In a frame (S') rotating with respect to the laboratory frame (S) with an angular velocity $\vec{\omega}$, the Eqn. 1.10 can be rewritten as

$$\frac{\partial \vec{\mu}}{\partial t} = \gamma \vec{\mu} \times (\vec{H} + \vec{\omega}/\gamma) \quad (1.12)$$

Equation 1.12 has the same form as Eqn. 1.11 provided the magnetic field H is replaced by an effective field $H_e = \vec{H} + \vec{\omega}/\gamma$. For a field $H = \vec{H}_o$ constant in time, the effective field H_e will vanish if a frame rotating with angular velocity $\omega_o = -\gamma H_o$ is chosen. In this frame $\partial \mu / \partial t = 0$, which means $\vec{\mu}$ is a constant vector. However, with respect to the laboratory frame (S), $\vec{\mu}$ is precessing with an angular velocity ω_o about the magnetic field \vec{H}_o . If the field \vec{H} is the sum of the constant field $\vec{H}_o = \omega_o \hat{k} / \gamma$ and a field \vec{H}_1 perpendicular to \vec{H}_o and rotating around it with an angular velocity $\vec{\omega}$, then the effective field in the rotating frame (S') is given as,

$$\vec{H}_o = (H_o + \omega/\gamma) \hat{k} + H_1 \hat{i} \quad (1.13)$$

In the rotating frame, the motion of the magnetic moment $\vec{\mu}$ is a Larmor precession around the effective field \vec{H}_e , of angular velocity $-\gamma\vec{H}_o$. The magnitude of the effective field \vec{H}_e can be written as

$$\vec{H}_o = \left[\left(\vec{H}_o + \vec{\omega}/\gamma \right)^2 + \vec{H}_1^2 \right]^{1/2} = -\frac{1}{|\gamma|} \left[(\vec{\omega}_o - \vec{\omega})^2 + \vec{\omega}_1^2 \right]^{1/2} \gamma = -a/\gamma . \quad (1.14)$$

The angle θ between \vec{H}_e and the applied field \vec{H}_o , which goes from 0 to π is given as

$$\tan \theta = \frac{\omega_1}{(\omega_o - \omega)} . \quad (1.15)$$

If at time $t=0$, the magnetic moment is aligned along \vec{H}_o , at a later time the angle between them will be

$$\cos \alpha = 1 - 2 \sin^2 \theta \sin^2 (at/2) . \quad (1.16)$$

From Eqns. 1.15 and 1.16, it can be seen that a rotating field \vec{H}_1 , generally small compared with the constant field \vec{H}_o can reorient appreciably a magnetic moment only if its frequency of rotation ω is in the neighbourhood of the Larmor frequency ω_o .

1.3 Quantum mechanical Picture- Spin Hamiltonian

The complete Hamiltonian H of a molecular system is in most cases enormously complex and the determination of exact solutions of the equation of motion for the entire quantum mechanical system is a very difficult task. Fortunately, magnetic resonance experiments can be described by a drastically simplified Hamiltonian called the ‘Spin Hamiltonian’. The nuclear spin Hamiltonian contains only nuclear spin operators and a few phenomenological constants that originate from the reduction process of the complete Hamiltonian. The Hamiltonian H for any particular spin system is the summation of individual Hamiltonians that describe particular interaction characterized by H_λ , and can be written as

$$H = \sum_{\lambda} H_{\lambda} . \quad (1.17)$$

In general the Hamiltonians can be divided into two classes: (1) H_{ext} : Hamiltonians that describe interactions of the spins with external fields. For example, magnetic interactions

of the nuclear spins with static external field (H_z) or with time dependent rf field (H_{RF}).
 (2) H_{int} : Hamiltonians that describe the direct and indirect interactions of the spins with internal fields. For example, dipolar (H_D), scalar (H_I) and quadrupolar Hamiltonian (H_Q) [3]. Here the Hamiltonians relevant to the work carried out in this thesis are described.

1.3.1 The Dipolar Hamiltonian H_D

The Dipolar Hamiltonian H_D for two nuclei (1 and 2) separated by a distance r can be written as

$$H_D = \frac{\mu_o \gamma_1 \gamma_2 \hbar^2}{4\pi} \left[\frac{\vec{I}_1 \cdot \vec{I}_2}{r^3} - \frac{3(\vec{I}_1 \cdot \vec{r})(\vec{I}_2 \cdot \vec{r})}{r^5} \right], \quad (1.18)$$

where \vec{I}_i is the spin angular momentum operator of nucleus i and γ_i is the gyromagnetic ratio of nucleus i (in $s^{-1}T^{-1}$). In matrix form the above equation can be written as

$$H_{DD} = hR \begin{pmatrix} \hat{I}_{1x} & \hat{I}_{1y} & \hat{I}_{1z} \end{pmatrix} \begin{pmatrix} \frac{r^2 - 3x^2}{r^2} & \frac{-3xy}{r^2} & \frac{-3xz}{r^2} \\ \frac{-3xy}{r^2} & \frac{r^2 - 3y^2}{r^2} & \frac{-3yz}{r^2} \\ \frac{-3xz}{r^2} & \frac{-3yz}{r^2} & \frac{r^2 - 3z^2}{r^2} \end{pmatrix} \begin{pmatrix} \hat{I}_{2x} \\ \hat{I}_{2y} \\ \hat{I}_{2z} \end{pmatrix}, \quad (1.19)$$

where $R = \frac{\gamma_1 \gamma_2 \mu_o \hbar}{r^3 4\pi 2\pi}$.

Equation 1.19 can be abbreviated and written as

$$H_{DD} = hR (\vec{I}_1 \cdot D \cdot \vec{I}_2), \quad (1.20)$$

where D is the direct dipolar tensor. If the internuclear vector \vec{r} lies along the z -axis, then the dipolar tensor becomes diagonal given by

$$D = \begin{pmatrix} 1 & 0 & 0 \\ 0 & 1 & 0 \\ 0 & 0 & -2 \end{pmatrix}. \quad (1.21)$$

This is called the principal axis system (PAS) of the dipolar tensor.

In order to discuss the NMR spectrum of two dipolar coupled spins in the solid state, generally Eqn. 1.19 is written in the spherical polar co-ordinate system as

$$H_{DD} = hR(A + B + C + D + E + F), \quad (1.22)$$

where

$$A = I_{1z}I_{2z} (1 - 3\cos^2 \theta),$$

$$B = -\frac{1}{4} (I_1^+ I_2^- + I_1^- I_2^+) (1 - 3\cos^2 \theta),$$

$$C = -\frac{3}{2} (I_1^+ I_{2z} + I_{1z} I_2^+) \sin \theta \cos \theta e^{-i\phi},$$

$$D = -\frac{3}{2} (I_1^- I_{2z} + I_{1z} I_2^-) \sin \theta \cos \theta e^{i\phi},$$

$$E = -\frac{3}{4} I_1^+ I_2^+ \sin^2 \theta e^{-2i\phi},$$

$$F = -\frac{3}{4} I_1^- I_2^- \sin^2 \theta e^{2i\phi}.$$

Each of the terms 'A' to 'F' contains a spin factor and a geometrical factor. The common factor hR is referred to as the dipolar coupling constant. If the eigenvalues of I_{1z} and I_{2z} are represented by m_1 and m_2 , the spin part of 'A' and 'B' terms connect states with $\Delta m = 0$, 'C' and 'D' terms connect states with $\Delta m = \pm 1$ and 'E' and 'F' terms connect states with $\Delta m = \pm 2$ where $\Delta m = m_1 - m_2$.

The terms 'C' to 'F' which produce very weak responses at $\omega = 0$ and $2\omega_0$ are neglected and hence do not contribute to the line width. The geometrical factors in Eqn. 1.22 are affected by molecular motions. Isotropic tumbling of the molecule averages out the terms A to F, to zero in the case of isotropic fluids and do not affect the transition energies or intensities for the high-resolution NMR spectra of isotropic fluids. However, dipolar interactions do affect the relaxation times even for isotropic solutions. If intramolecular interactions are considered, molecular tumbling will modulate terms 'C' to 'F', which will result in spin-lattice relaxation.

1.3.2 Method of moments

Line shape study is an important tool in the analysis of molecular and crystal structure. Theoretical line shape for a two spin system has been solved by Pake [4 - 5], three spin and four spin systems have also been analysed by several other authors [6 – 11]. The ^1H NMR spectrum of symmetric molecular subgroups like NH_4 , $\text{N}(\text{CH}_3)_4$, CH_3 and NH_3 , contain characteristic, symmetrically disposed lines about the central line depending on the size and shape of the molecular subgroups. The interaction between the nuclear spins of the neighboring molecular groups causes broadening in these lines and removes the structural details in the spectrum, making the task of calculating the line shape formidable. In such cases, Van Vleck (12) has shown that the second moment of the spectrum can be profitably used to get information about the structure and dynamics.

In general, the n^{th} moment of a line shape $f(\omega)$ about ω_0 is given by

$$M_n = \frac{\int_0^{\infty} (\omega - \omega_0)^n f(\omega) d\omega}{\int_0^{\infty} f(\omega) d\omega}, \quad (1.23)$$

where ω is the spectral coordinate in frequency units. If the absorption line is symmetric about ω_0 , all odd moments about the center of the line vanish. The second moment of a line is just the mean square line width and is given by

$$M_2 = \frac{\left(\int_0^{\infty} \Delta\omega^2 f(\omega) d\omega \right)}{\left(\int_0^{\infty} f(\omega) d\omega \right)}, \quad (1.24)$$

where $\Delta\omega = (\omega - \omega_0)$. The absorption line observed in diamagnetic solids is normally Gaussian and is characterized by its second moment. Second moment contains line broadening contributions from pair-wise interaction between spins. The effect of multispin correlations is given by the higher moments.

The Hamiltonian is truncated to exclude the satellite lines which are far removed from resonance and too weak to be observed. Despite the small magnitude of $f(\omega)$ for the satellites in Eqn. 1.24, the magnitude of the term $(\omega - \omega_0)^2$ produces a large contribution to the integral $\langle (\omega - \omega_0)^2 \rangle$. Van Vleck's calculations show that the overall second moment, including satellites, is 10/3 times the second moment of the main line. Thus the satellite lines contribute 7/3 times the contribution from the main line to the second moment. To avoid erroneous comparison with the observed second moment, the truncated Hamiltonian is used in calculation of the theoretical second moment.

For a polycrystalline sample, the rigid lattice second moment is given by the Van Vleck expression [4]

$$M_{2RL} = \langle \Delta\omega^2 \rangle_{RL} \propto \overline{(1 - 3\cos^2\theta_{ij})^2}, \quad (1.25)$$

where θ_{ij} is the angle between the static magnetic field H_0 and the inter-nuclear vector r_{ij} as shown in the Fig. 1.2. The bar indicates the average over θ_{ij} . Van Vleck's expression for the second moment in terms of the coordinates of the nuclei is

$$\langle \Delta\omega^2 \rangle = \left(\frac{3}{4}\right) \left(\frac{I(I+1)\gamma^4\hbar^2}{N}\right) \sum_{i<j} \left(\frac{\mu_i^2}{r_{ij}^6}\right), \quad (1.26)$$

where $\mu_i = (1-3\cos^2\theta_{ij})$, γ is the nuclear gyromagnetic ratio of spin I and N is the number of spins in the system at resonance.

For polycrystalline sample, the isotropic average of $(1-3\cos^2\theta_{ij})$ reduces to 4/5. Thus the expression for second moment, for identical spins, becomes

$$\langle \Delta\omega^2 \rangle = \left(\frac{3}{5}\right) \left(\frac{I(I+1)\gamma^4\hbar^2}{N}\right) \sum_j \left(\frac{1}{r_j^6}\right). \quad (1.27)$$

However, experimentally the second moment M_2 of the absorption line is obtained by numerical integration of the observed first derivative using the expression

$$M_2 = \frac{1}{3} \frac{\int_0^{\infty} (\Delta\omega)^3 f'(\omega) d\omega}{\int_0^{\infty} (\Delta\omega) f'(\omega) d\omega}, \quad (1.28)$$

where $\Delta\omega = (\omega - \omega_0)$, is the deviation from the center of the resonance line and $f'(\omega)$ is the amplitude of the derivative signal at ω .

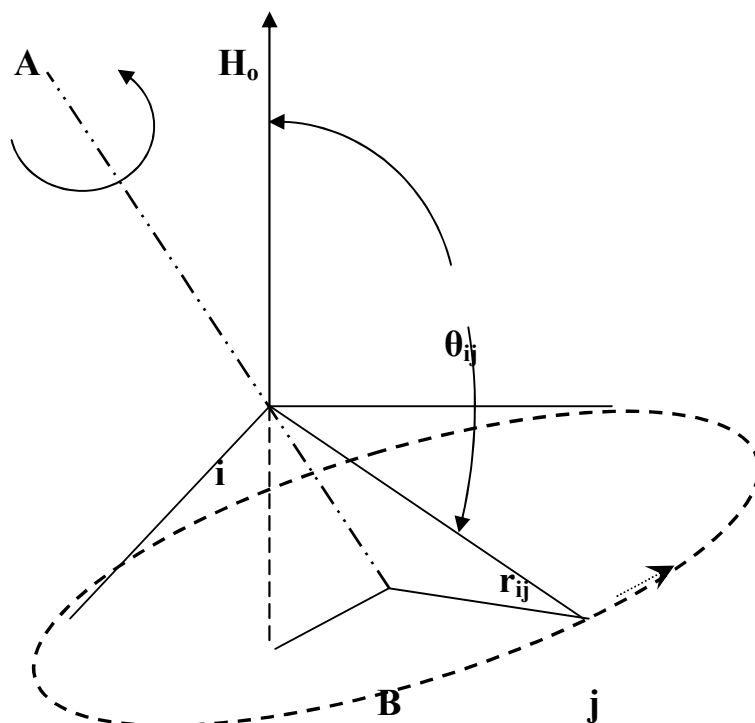


Figure 1.2 Motion of an inter-proton vector r_{ij} about an axis AB.

In the presence of molecular motion (reorientation of the symmetric groups), it is observed that the central portion of the absorption line is narrowed and the wings are broadened. However, it should be noted that the total second moment of a line does not change, but only the observed second moment changes. The observable part of the second moment decreases due to molecular motions.

1.4 Effects of molecular Motion

1.4.1 Line Narrowing

In many solids, there is often considerable motion of the whole molecule or molecular sub-groups about their symmetry axes. As mentioned earlier, we are interested in diamagnetic solids containing symmetric proton groups like NH_4 , CH_3 and $\text{N}(\text{CH}_3)_4$. In such systems, line shape and broadening are determined mainly by dipole-dipole interaction. Molecular motions, which are fast compared to the line width, reduce the width of the resonance lines. If τ_c is the correlation time of the fluctuations and M_2 is the second moment, then the line narrowing occurs when $(M_2)^{1/2} \tau_c \ll 1$, where $(M_2)^{1/2}$ can be regarded as a measure of the line width.

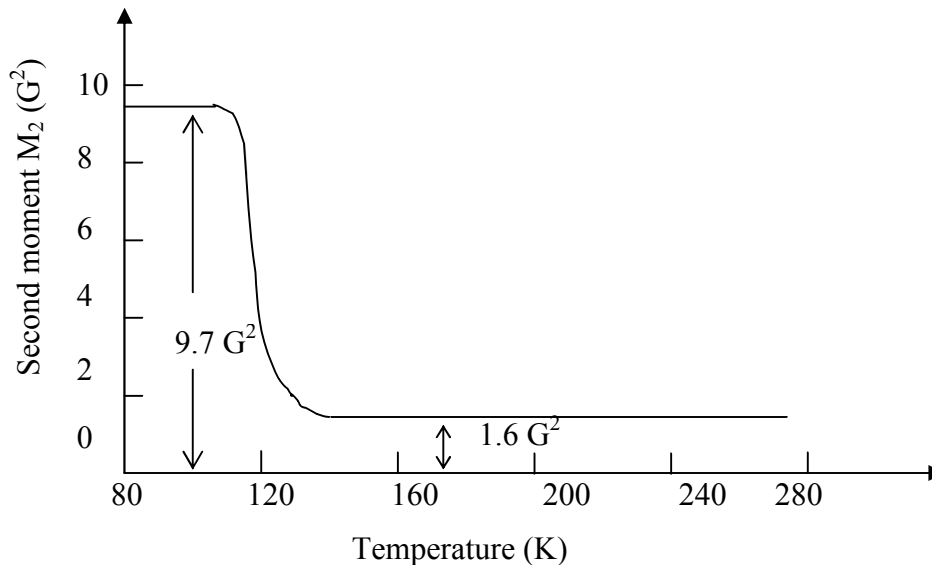


Figure 1.3 Variation of second moment with temperature in solid benzene [13].

At sufficiently low temperatures, these internal motions are inhibited ($\tau_c^{-1} \ll (M_2)^{1/2}$) and the second moment attains a rigid lattice value (M_{2RL}). From a study of the temperature dependence of line width or second moment, the motional parameters like correlation time and activation energy can be determined using the expression [4]

$$M_{2R} = M_{2HT} + M_{2RL} \left[\left(\frac{2}{\pi} \right) \tan(\alpha) (M_2)^{1/2} \tau_c \right], \quad (1.29)$$

and the Arrhenius equation

$$\tau_c = \tau_o \exp\left(\frac{E_a}{k_B T}\right) \quad (1.30)$$

Here α is a numerical factor of the order of unity, M_{2R} is the resultant second moment and E_a is the activation energy. However, second moment studies can provide information on the motional parameters only over a limited temperature range, over which the second moment transition occurs. A typical example to elucidate this variation of second moment is shown in Fig. 1.3 for solid benzene [13].

1.4.2 Relaxation

The spin lattice relaxation involves an energy exchange between the spin system and the lattice. The following are some of the interactions, which can cause spin-lattice relaxation: (1) magnetic dipole-dipole interaction, (2) translational diffusion, (3) spin rotation interaction and (4) quantum rotational tunnelling. If these interactions have fluctuations at the Larmor frequency (ω_o), they can cause spin-lattice relaxation. The spin-lattice relaxation time (T_1) depends upon the magnitude and the rate of fluctuations of these interactions.

1.4.2.1 Dipole-dipole interaction

In diamagnetic solids (in the absence of quadrupole interactions), spin lattice relaxation is mainly caused by modulation of the dipole-dipole interaction caused by the internal motions. Since the magnetic dipole-dipole interaction is mainly responsible for the relaxation in all our studies, the procedure to arrive at an expression for spin-lattice relaxation rate ($1/T_1$) due to this interaction (both between like spins and unlike spins) first derived by Bloembergen-Purcell and Pound (BPP) [14], using operator mechanism, is given below.

The dipole-dipole interaction between two spins I and I' can be written as [3]

$$\hbar H_1 = \sum_q F^q A^q, \quad (1.31)$$

where the F^q are random functions of time and the A^q are operators acting on the spin variables with the convention $F^q = F^{-q}$; $A^q = A^{-q}$. $F^q(t)$ can be characterized by the

auto-correlation function $G(\tau)$ which is an even and real function of the correlation time τ and can be written as

$$G(\tau) = \overline{F(t)F(t+\tau)}, \quad (1.32)$$

where the bar represents an ensemble average.

The Fourier transform of $G(\tau)$ is the spectral density denoted by

$$J(\omega) = \int_{-\infty}^{\infty} G(\tau) \exp(-i\omega\tau) d\tau. \quad (1.33)$$

If it is assumed that the correlation function is represented by $\exp\left(-\frac{|\tau|}{\tau_c}\right)$ [14],

where τ_c is called the correlation time characteristic of the random motion, then the spectral density function can be written as

$$J(\omega) = \frac{2\tau_c}{1 + \omega^2\tau_c^2}. \quad (1.34)$$

The above expression says that for a given frequency ω , $J(\omega)$ is maximum for $\tau_c = \frac{1}{\omega}$. Therefore, for a constant power available in the relaxation spectrum, the rate of relaxation transition induced is a maximum when the correlation time is of the order of $\frac{1}{\omega}$ (the Larmor period). $J(\omega)$ decreases and becomes zero for both very shorter and longer τ_c compared with $\frac{1}{\omega}$. Figure 1.4 shows a schematic picture of the spectral density as a function of ω . It can be seen that the power spectrum has a cut-off for a frequency $\omega_o = \frac{1}{\tau_c}$ and is uniform for $\omega < \omega_o$. If ω is much smaller than the Larmor frequency ω_o , then there is no power available for the transition and the relaxation rate $\frac{1}{T_1}$ is very small. If $\omega < \omega_o$, the power spectrum is spread uniformly over a very large band and since its total intensity is constant, $J(\omega)$ and $\frac{1}{T_1}$ will accordingly be small. An optimum condition exists for an intermediate value of $\omega_o \sim \frac{1}{\tau_c}$.

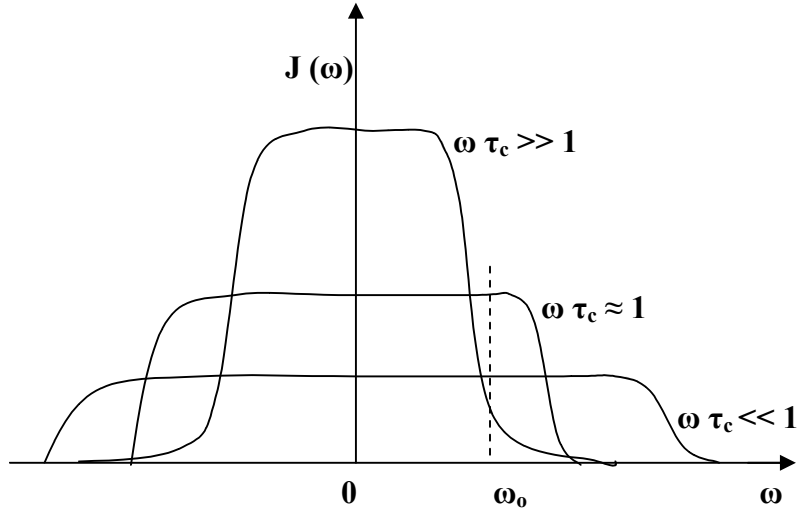


Figure 1.4 Distribution of spectral density as a function of frequency.

The random fluctuations are written as

$$\begin{aligned}
 F^1 &= \frac{\sin\theta \cos\theta e^{-i\phi}}{r^3}, \\
 F^2 &= \frac{\sin^2\theta e^{-2i\phi}}{r^3}, \\
 F^0 &= \frac{(1 - 3\cos^2\theta)}{r^3},
 \end{aligned} \tag{1.35}$$

where ‘r’ is the inter-nuclear distance, A^q 's which are the operators acting on the system are given as

$$\begin{aligned}
 A^0 &= \alpha \left(\frac{-2}{3} I_z I'_z + \frac{I_+ I'_- + I_- I'_+}{6} \right), \\
 A^1 &= \alpha (I_z I'_+ + I_+ I'_z), \\
 A^2 &= \frac{\alpha I_+ I'_+}{2},
 \end{aligned} \tag{1.36}$$

where $\alpha = -\frac{\gamma_I \gamma_{I'} \hbar}{2}$.

The starting point to arrive at an expression for the relaxation rate is to know the rate of change of magnetisations namely I_z and I'_z with time. It has to be noticed that if

the spins \vec{I} and \vec{I}' are like spins only the sum $\langle \vec{I} \rangle + \langle \vec{I}' \rangle$ is observed, where as $\langle \vec{I} \rangle$ and $\langle \vec{I}' \rangle$ are observed separately if the spins are unlike.

Like spins

The main Hamiltonian $\hbar H_o$ in the case of like spins is given by

$$\hbar H_o = \hbar \omega_0 (I_z + I'_z). \quad (1.37)$$

the equation of motion of the longitudinal magnetization which is proportional to $\langle \vec{I} \rangle + \langle \vec{I}' \rangle$ can be written in the form

$$\frac{d(\langle \vec{I} \rangle + \langle \vec{I}' \rangle)}{dt} = -(a_z - a_o). \quad (1.38)$$

In Eqn. 1.38, $a_z = \text{Tr} (A_z \sigma^*)$ and

$$A_z = \frac{1}{2} \sum_{qp} J_q (\omega_p^q) [A_p^q, [A_p^{-q}, I_z + I'_z]]$$

$$\sigma^*(t) = \exp(i H_o t) \sigma(t) \exp(-i H_o t)$$

where $\sigma(t)$ is the average density operator of the system. For the case of dipolar coupling between two spins, A_z can be written as

$$A_z = \frac{1}{2} J^1(\omega_I) ([A^{-1}, [A^1, I_z + I'_z]]) + h.c. + \frac{1}{2} J^1(2\omega_I) ([A^{-2}, [A^2, I_z + I'_z]]) + h.c. \quad (1.39)$$

where 'h.c.' denotes the Hermitian conjugate [3]. The commutators can be evaluated using the standard angular momentum commutation relations and in the high temperature approximation one finally gets

$$\langle A_z \rangle \cong \frac{2\alpha^2}{3} I(I+1) \langle I_z + I'_z \rangle (J^1(\omega_I) + J^2(2\omega_I)). \quad (1.40)$$

Now Eqn 1.38 can be written as

$$\frac{d\langle \bar{I} + \bar{I}' \rangle}{dt} = -\frac{1}{T_1} \left(\langle \bar{I} + \bar{I}' \rangle - \langle \bar{I} + \bar{I}' \rangle_o \right), \quad (1.41)$$

with

$$\frac{1}{T_1} = \frac{3}{2} \gamma^4 \hbar^2 I(I+1) \left(J^1(\omega_I) + J^2(2\omega_I) \right). \quad (1.42)$$

Using the expression for the spectral density, Eqn. 1.42 can be written as

$$\frac{1}{T_1} = \frac{3}{2} \frac{\gamma^4 \hbar^2 I(I+1)}{r^6} \left(\frac{\tau_c}{1 + \omega_I^2 \tau_c^2} + \frac{4\tau_c}{1 + 4\omega_I^2 \tau_c^2} \right) \quad (1.43)$$

Eqn. 1.43 is generally known as the BPP equation. This equation is used widely in the investigations reported in this thesis.

Unlike Spins

The main Hamiltonian in the case of unlike spins is given by

$$\hbar H_o = \hbar \left(\omega_I I_z + \omega_S I'_z \right). \quad (1.44)$$

As mentioned previously, in the case of unlike spins, one has to write the equations of motion of $\langle I \rangle$ and $\langle S \rangle$ separately as $\langle I \rangle$ and $\langle S \rangle$ are observed separately. Proceeding similarly as in the case of like spins, we get

$$\begin{aligned} \langle A_z^I \rangle &= \gamma_I^2 \gamma_S^2 \hbar^2 \langle I_z \rangle S(S+1) \left[\frac{J^0(\omega_I - \omega_S)}{12} + \frac{3}{2} J^1(\omega_I) + \frac{3}{4} J^2(\omega_I + \omega_S) \right] \\ &+ \gamma_I^2 \gamma_S^2 \hbar^2 \langle S_z \rangle I(I+1) \left[\frac{-J^0(\omega_I - \omega_S)}{12} + \frac{3}{4} J^2(\omega_I + \omega_S) \right]. \end{aligned} \quad (1.45)$$

An identical equation is obtained for $\langle A_z^S \rangle$ by interchanging the spins I and S. Finally the rate of change of magnetizations $\langle I_z \rangle$ and $\langle S_z \rangle$ can be written as

$$\frac{d\langle I_z \rangle}{dt} = -\frac{1}{T_1^{II}} (\langle I_z \rangle - I_o) - \frac{1}{T_1^{IS}} (\langle S_z \rangle - S_o) , \quad (1.46)$$

$$\frac{d\langle S_z \rangle}{dt} = -\frac{1}{T_1^{SI}} (\langle I_z \rangle - I_o) - \frac{1}{T_1^{SS}} (\langle S_z \rangle - S_o) . \quad (1.47)$$

From these equations, it follows that

$$\begin{aligned} \frac{1}{T_1^{II}} &= \gamma_I^2 \gamma_S^2 \hbar^2 S(S+1) \left[\frac{1}{12} J^0(\omega_I - \omega_S) + \frac{3}{2} J^1(\omega_I) + \frac{3}{4} J^2(\omega_I + \omega_S) \right] \\ \text{and} \quad \frac{1}{T_1^{IS}} &= \gamma_I^2 \gamma_S^2 \hbar^2 I(I+1) \left[-\frac{1}{12} J^0(\omega_I - \omega_S) + \frac{3}{4} J^2(\omega_I + \omega_S) \right]. \end{aligned} \quad (1.48)$$

Similar equation can be obtained for $\frac{1}{T_1^{SS}}$ and $\frac{1}{T_1^{SI}}$ by interchanging the indices I and S. It is important to note from Eqns 1.46 and 1.47 that the polarization of the spins I and S are coupled so that radio frequency field at frequency ω_I will affect $\langle S_z \rangle$ while acting upon $\langle I_z \rangle$.

For thermally activated random processes, the temperature dependence of the correlation time is given any the Arrhenius equation [14]

$$\tau_c = \tau_o \exp\left(\frac{E_a}{k_B T}\right), \quad (1.49)$$

where E_a is the activation energy for the thermal process, k_B is the Boltzmann constant, T is the absolute temperature and τ_o , the pre-exponential factor, is the correlation time at infinite temperature. At low temperatures when $\omega\tau \gg 1$

$$\frac{1}{T_1} = \frac{2C}{\omega_o^2 \tau_c^2} . \quad (1.50)$$

At high temperatures when $\omega\tau \ll 1$

$$\frac{1}{T_1} = 5C \tau_c . \quad (1.51)$$

At intermediate temperatures when $\omega\tau = 0.69$, T_1 exhibits a minimum and its value

is given by

$$\frac{1}{T_{1\min}} = C \frac{1.42}{\omega_o} \quad (1.52)$$

In these equations, ‘C’ is the relaxation constant given by

$$C = \frac{3}{2} \frac{\gamma^4 \hbar^2 I(I+1)}{r^6} \quad (1.53)$$

$$\text{and} \quad C = \frac{3}{2} \frac{\gamma_I^2 \gamma_S^2 \hbar^2 I(I+1)}{r^6} \quad (1.54)$$

Eqn 1.53 gives the relaxation constant in the case of dipolar interaction between like spins and Eqn 1.54 gives the relaxation constant in the case of dipolar interaction between unlike spins. ‘r’ is the inter-nucleus distance and the other symbols have been explained before.

By measuring the spin-lattice relaxation time (T_1) as a function of temperature, the motional parameters namely the pre-exponential factor and the activation energy for the relevant molecular motion can be determined.

1.4.2.2 Translational diffusion

Intra-molecular and inter-molecular interactions between the spins are responsible for relaxation. Intra-molecular interactions are modulated by reorientational motion while inter-molecular interactions are modulated by both translational motion as well as the rotation motion. In some solids, it is experimentally observed that, the line width becomes extremely narrow at higher temperatures, which cannot be explained based on motional averaging of the intra-molecular dipole-dipole interaction. A treatment of translational diffusion explains this behaviour. Bloembergen et al [14] and Torrey [15] together proposed a model using random walk method for translational diffusion of ions through lattice and this is well explained in Abragam [3].

The coefficient of diffusion given by the Stokes formula is [3]

$$D = \left(\frac{kT}{6\pi a\eta} \right), \quad (1.55)$$

where 'a' is the distance of closest approach, k is the Boltzman constant and η is the coefficient of viscosity at temperature T (K).

Similarly, the translational diffusion theory developed to explain the relaxation can be represented as [15, 16]

$$\frac{\partial \psi (r, t)}{\partial t} = D \Delta \Psi ,$$

where 'D' is the coefficient of diffusion. The solution of the above diffusion equation is

$$\Psi (r, r_o, t) = (4\pi Dt)^{-3/2} \exp \left(-\frac{(r-r_o)^2}{4Dt} \right) \quad (1.56)$$

In Eqn. 1.56, vector 'r' represents the distance (r_1-r_2) between two identical molecules, which diffuse relative to each other and 'r_o' is the equilibrium separation between them. Taking the relative displacements of molecules as $2D t$ instead of Dt (to prevent the spectral intensities $J_i(\omega)$ from becoming infinite), the effective motion can be represented by the equation

$$\Psi(r, r_o, t) = (8\pi Dt)^{-3/2} \exp \left(-\frac{(r-r_o)^2}{8Dt} \right) . \quad (1.57)$$

The limiting value of 'r' and 'r_o' is d, the diameter of the molecule. This is the least distance of approach of the molecules. If the molecules are spherical, then $d = 2a$, where 'a' is the molecular radius. Considering these aspects, the expression obtained for correlation time can be written as

$$G(t) = \left(\frac{N}{d^3} \right) \int_0^\infty [J_{3/2}(u)]^2 \exp \left(-\frac{2Du^2t}{d^2} \right) \left(\frac{du}{u} \right) , \quad (1.58)$$

where $u = \rho d$; ρ is the orientation vector relating ($r-r_o$) and $J(u)$ is the Bessel function. The Fourier transform of this correlation function gives the spectral density as

$$J(\omega) = \left(\frac{N}{dD} \right) \int_0^{\infty} \frac{[J_{3/2}(u)]^2}{u^3} \left(\frac{du}{1 + (\omega^2 \tau^2 / u^4)} \right) = \left(\frac{N}{dD} \right) \int_0^{\infty} [J_{3/2}(u)]^2 \left[\frac{u du}{(u^4 + \omega^2 \tau^2)} \right]. \quad (1.59)$$

The correlation time for this kind of motion is given by

$$\tau = \left(\frac{12 \pi a^3 \eta}{k T} \right) = 9 \tau_2, \quad (1.60)$$

where τ_2 is the correlation time for spin rotation mechanism and this equation is applicable for the homogeneous medium. For an inhomogeneous medium this equation has to be modified [17]. At higher temperature where diffusion is active, $\omega \tau \ll 1$. Thus the term $(1 + (\omega^2 \tau^2 / u^4))$ reduces to unity and the integral reduces to (2/15) and hence

$$J(0) = \left(\frac{2 \pi N \eta}{5 k T} \right). \quad (1.61)$$

Here N represents the density of spins per cubic centimeter. Similarly, it can be shown that [15]

$$J(1) = \left(\frac{8 \pi}{15} \right) J(0) \quad (1.62)$$

$$\text{and} \quad J(2) = \left(\frac{32 \pi}{15} \right) J(0). \quad (1.63)$$

Hence, Considering these factors the relaxation rate due to translational diffusion can be written as [3, 15]

$$T_{1td}^{-1} \propto J(\omega) = \left(\frac{3}{2} \right) I(I+1) \gamma^4 \hbar^2 [J(1) + J(2)] \quad (1.64)$$

and hence it can also be represented as

$$T_{1td}^{-1} = \left(\frac{8\pi N}{15a^3} \right) I(I+1)\gamma^4 \hbar^2 \left[\frac{\tau/2}{1 + (\omega\tau/2)^2} + \frac{\tau}{1 + \omega^2\tau^2} \right]. \quad (1.65)$$

1.4.2.3 Tunnelling reorientation

Many organic compounds containing symmetric groups have shown additional minima in the low temperature region of the plots of T_1 versus temperature along with classical minima [18 - 22]. In some compounds, T_1 exhibits minima only at lower temperatures, without showing classical minima at higher temperatures. Also, some systems have shown finite T_1 value (\sim ms) at lower temperatures, exhibiting a temperature independent down to helium temperatures [20]. This behaviour has been assigned to quantum rotational tunnelling.

In solids, both inter and intra-molecular forces constrain molecules and their internal groups to certain equilibrium positions related to their symmetry. When the hindering potential is quite low, the molecules exist in a number of torsional oscillator states. A coupling of the torsional oscillator states to the rest of the lattice exists which leads to a Boltzmann distribution of population among the torsional oscillator levels.

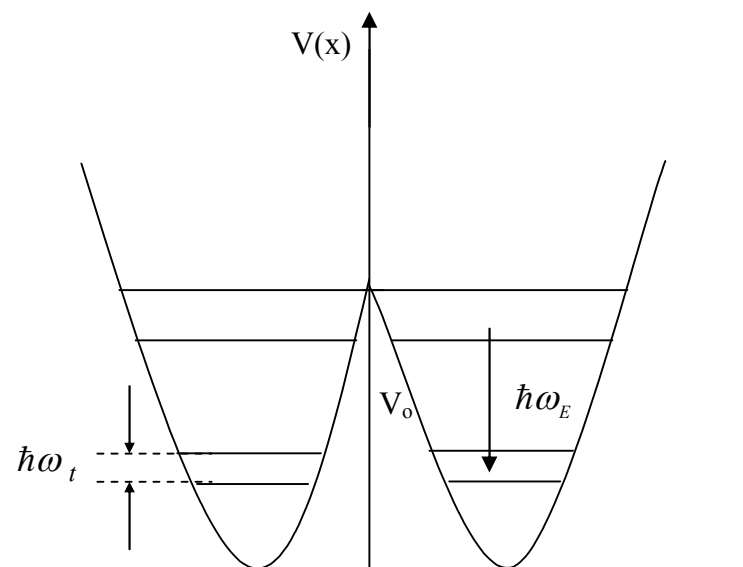


Figure 1.5 A schematic diagram of the tunnelling process in a two-level system.

When the atoms of a molecule can exist in configurations which are distinct and yet energetically identical, the molecule can flip (hopping from ground torsional state of one potential well to a free rotor state and then to the torsional state in another but equivalent potential well) from one configuration to the other, if it is supplied with sufficient energy to surmount the barrier between the configurations. This kind of hopping or random reorientation over the barrier height is a thermally activated process governed by the classical Arrhenius relationship and is efficient only at temperatures high enough in relation to the activation energy E_a [23]. It is well known from quantum mechanics that, the wave function of a particle is not confined only in its potential well, but there is a finite probability of the molecule changing from one configuration to another without being supplied the energy to surmount the barrier. Normally, effects due to such tunnelling will be observable at low temperatures where effects of random reorientations due to thermal energy possessed by the molecules is suppressed sufficiently [24].

For the harmonic potential, the tunnelling frequency is

$$\omega_t = 2\omega_E \left[\frac{2V_o}{\hbar\omega_E\pi} \right]^{1/2} \exp \left[\frac{-2V_o}{\hbar\omega_E} \right] \quad \text{for } V_o > \hbar\omega_E$$

where V_o is the barrier height and $\hbar\omega_E$ is the separation between successive pairs of energy levels corresponding to the harmonic oscillator frequency. ω_t depends on the ratio of the barrier height to the oscillator energy. Hund [25] showed that for $\hbar\omega_E = 1000 \text{ cm}^{-1}$, the tunnelling period ranges from 10^{-9} to 10^9 years for a variation $\left[\frac{2V_o}{\hbar\omega_E} \right]$ from 10 to 70. Although this is a case of translational tunnelling, its essential features are the same as for rotational tunnelling. It must be noted that a particle tunnelling between two equilibrium positions is meaningful only if initially (and at any other point of time) it is possible to find it sufficiently well localized in one of its equilibrium positions. The existence of this tunnel splitting was verified by microwave absorption measurements. Fig 1.5 shows the case of tunnelling in a two-well potential.

The general features of the tunnelling in NMR experiments are (a) structures in the NMR line shape (b) finite second moment value of the NMR absorption line compared to that of the rigid lattice value and (c) non-exponential behaviour in the magnetization recovery profile. In addition, another prominent and well-noticed feature of tunnelling is the occurrence of additional minima in the plot of spin lattice relaxation time (T_1) as a function of temperature (T) at much lower temperatures along with or without classical minima at higher temperatures.

Quantum rotational tunnelling of symmetric groups like NH_4 and CH_3 has been observed in many samples using NMR technique [26-32]. In addition, some efforts have been made to study the effect of isotope dependence on tunnelling by Lalowicz et al [33], Cavagnat [34], Ingman [35], Heuer [36] and recently by Latonowicz et al [37]. NMR line shapes show extra peaks corresponding to tunnelling sidebands [38]. Theoretical models were proposed mainly by Haupt [39], Punkkinen [40] and Clough [41] to explain the tunnelling of the CH_3 and NH_4 groups. However, these models could not explain the temperature dependence of the T_1 in the entire temperature range and also the value of the $T_{1\text{min}}$ at low temperatures. Sobol et al [42] attempted to fit the T_1 data in the entire temperature range using TART (Tunnelling Assisted Relaxation Theory) model and found discrepancy between the predictions and the experiment in the level crossing matching regions. They have also carried out frequency dispersion studies to find out the dependence of the tunnel frequency on the Larmor frequency. In $\text{Ge}(\text{CH}_3)_4$, the temperature dependence of the fast relaxation spectral line indicates that the Zeeman tunnelling relaxation processes cannot be the result of random thermally activated modulations [43, 44].

1.5 Free induction Decay

At thermal equilibrium and at time $t=0$, in the presence of an applied dc field H_0 , the sample containing the nuclear spins has a magnetization $M_z(0)$ parallel to the applied

dc field and is given by $M_z(0) = \chi_0 H_0$,

where χ_o is the susceptibility of the nuclei which can be written as

$$\chi_o = \frac{N \gamma^2 \hbar^2 I(I+1)}{3k_B T} . \quad (1.67)$$

Here N is the number of nuclear spins per unit volume of the sample, γ is the gyromagnetic ratio of the sample, I is the nuclear spin quantum number, k_B is the Boltzmann constant and T is the temperature of the sample.

There will not be any transverse magnetization in the sample at thermal equilibrium and at time $t = 0$. Such a magnetization can be created by applying a rotating field H_1 for a time τ and its frequency being equal to the Larmor frequency ω_o . After the application of the radio frequency pulse, the magnetization along the applied dc field, $M_z(\tau)$ and that perpendicular to the applied dc field, $M_+(\tau)$ can be written as [3]

$$M_z(\tau) = M_z(0) \cos(\omega_1 \tau) , \quad (1.68)$$

$$\text{and} \quad M_+(\tau) = M_z(0) \sin(\omega_1 \tau) \exp(i\omega_o \tau) \quad (1.69)$$

After the radio frequency field is cut off, there results a precessing magnetization given by

$$M_+(t) = M_z(0) \sin(\omega_1 \tau) \exp(i\omega_o t) . \quad (1.70)$$

The amplitude of the precessing magnetization $M_+(t)$ given in Eqn. 1.70. It becomes maximum when $\omega_1 \tau = \pi/2$ and this is called a 90° pulse. The precessing magnetization in the xy-plane vanishes when $\omega_1 \tau = \pi$ and this is called a 180° pulse. The precessing magnetization induces a voltage at the larmor frequency in the NMR sample coil which is picked up and detected and is known as the “free induction” signal. The precessing magnetization, after some time, decays due to various reasons such as inhomogeneity of the dc magnetic field, the interaction between the nuclear spins etc. and this decaying signal is generally referred to as the “Free Induction Decay”(FID) signal.

1.6 Measurement of M_2 and T_1

1.6.1 Second moment (M_2)

The Wide line NMR absorption signal is acquired onto the computer through a ADC interface as described in the section 2.2.4 (Chapter 2). The derivative signal is acquired onto the computer over certain scan time, by keeping the frequency of the oscillator constant and varying the static magnetic field over certain range around the vicinity of the signal (using auto sweep facility) for the same scan time. The acquired signal is further processed and second moment is evaluated using the numerical integration method using the software ORIGIN (version 7.5).

1.6.2 Spin lattice relaxation time (T_1)

T_1 can be measured in various ways depending on the convenience and sample. The basic principle of measuring the SLR time is first to set certain initial condition (value of magnetization at $t = 0$) of the spin system by applying a pulse sequence, known as preparation pulses. Then the spin system is allowed to evolve under the influence of H_0 and subsequently the fraction of the magnetization which has relaxed back to the z -direction is detected by another pulse, which is known as monitoring pulse. Different methods used for measurement of T_1 in our experiments are presented here. Figure 1.6 shows different steps of growth of magnetization after the application the $\pi/2$ pulse.

1.6.2.1 Inversion Recovery Method ($\pi - \tau - \pi/2$)

In this method, the maximum excursion from equilibrium is obtained by inverting the z -magnetization with a selective or non-selective π pulse [45] (an RF pulse, that rotates the magnetization vector by 180°). The recovery towards equilibrium is sampled after a delay τ by a $\pi / 2$ pulse, which creates transverse magnetization. For systems with isolated spins, one can write

$$M_z(\tau) = M_0 \left[1 - 2e^{-\frac{\tau}{T_1}} \right] \quad (1.71)$$

The equilibrium magnetization M_0 and spin lattice relaxation time T_1 have to be determined by monitoring the M_z as a function of delay τ . In some cases, where an ideal π pulse cannot be defined, one has to rewrite the Eqn. 1.71 as

$$M_z(\tau) = M_z(t=0) e^{-\frac{\tau}{T_1}} + M_0 \left[1 - e^{-\frac{\tau}{T_1}} \right]. \quad (1.72)$$

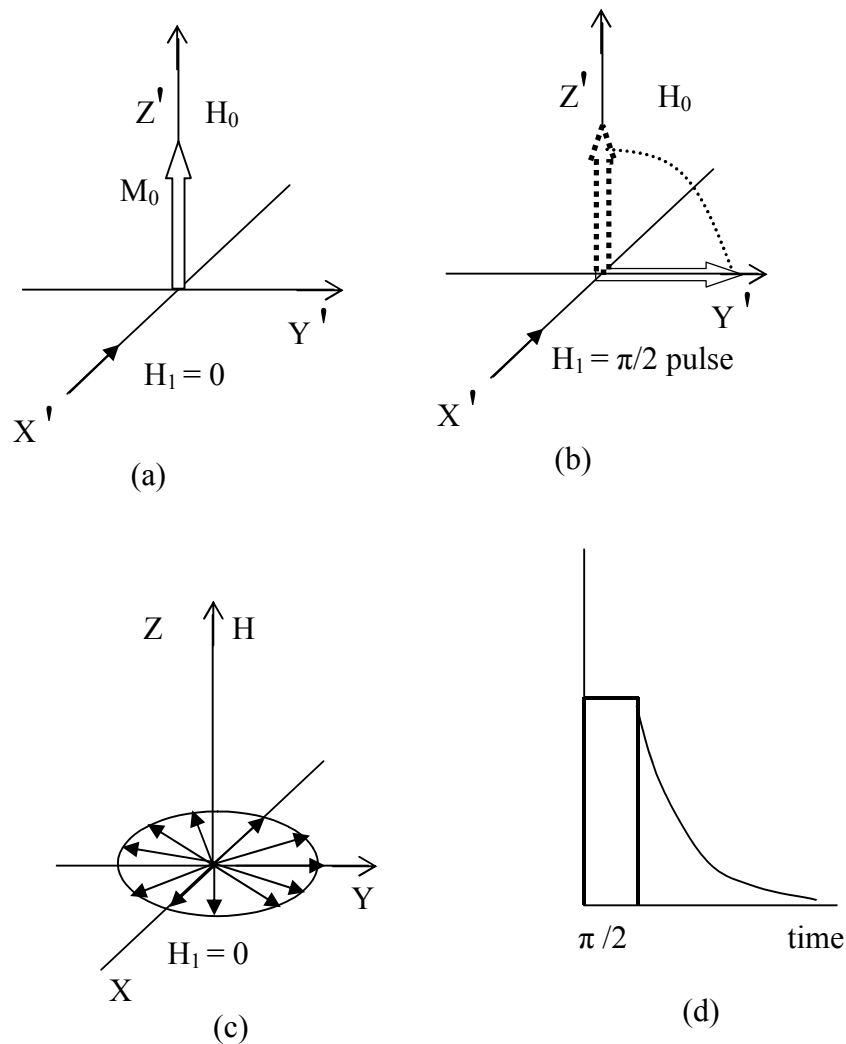


Figure 1.6 (a) Equilibrium magnetization M_0 when external rf field $H_1 = 0$
 (b) $\pi/2$ pulse tips M_0 along Y axis
 (c) Spin-spin relaxation process (dephasing of the spins)
 (d) Free induction decay (FID)

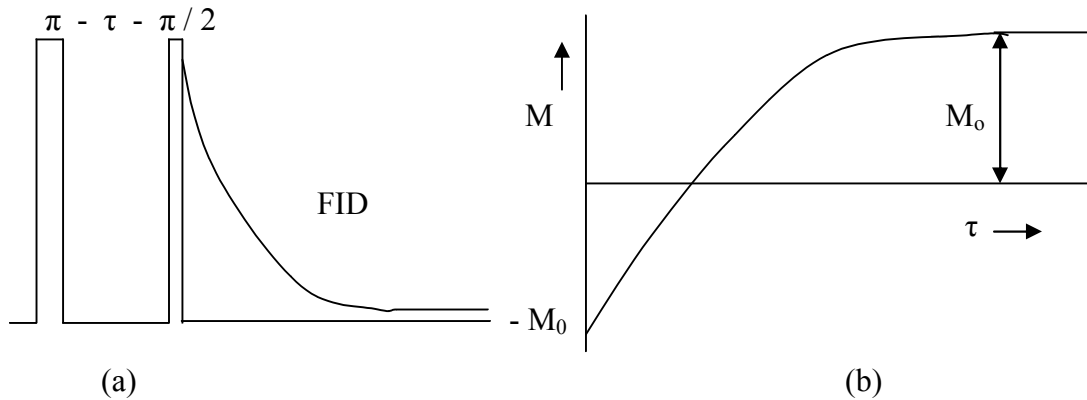


Figure 1.7 (a) The inversion recovery pulse sequence (b) the growth of magnetization, as function of ' τ '.

In this case, three parameters have to be determined for an isolated spin: the equilibrium magnetization M_0 , the initial magnetization after the inversion pulse $M_z(t = 0)$ and the spin lattice relaxation time T_1 .

Figure 1.7 shows the inversion recovery pulse sequence and the evolution of the magnetization recovery. T_1 is experimentally determined by measuring M_z at various values of ' τ ' and fitting that data to the Eqn. 1.71 using non-linear least square fit with two or three fit parameters. In the present investigations, ORIGIN (Version 7.5) is used for this purpose. This pulse sequence is generally used when T_1 is less than 1 sec.

1.6.2.2 Saturation Burst method

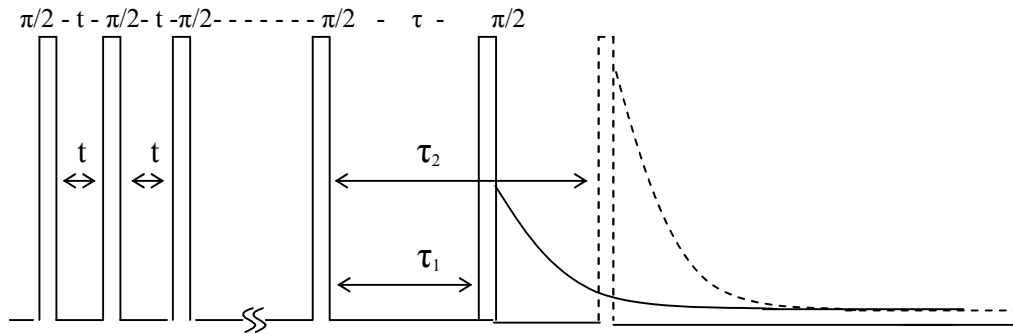
In this method, M_z is brought to the transverse plane by a comb of n $\pi/2$ pulses, then the growth of M_z back along the z -direction is monitored by another $\pi/2$ pulse as a function of the delay (τ) between the comb and the monitoring pulse. The separation of the pulses in the comb has to be greater than the dephasing time of the spins in the transverse plane. The magnetization in the transverse plane is given as

$$M_z(\tau) = M_0 \left[1 - e^{-\frac{\tau}{T_1}} \right] \quad (1.73)$$

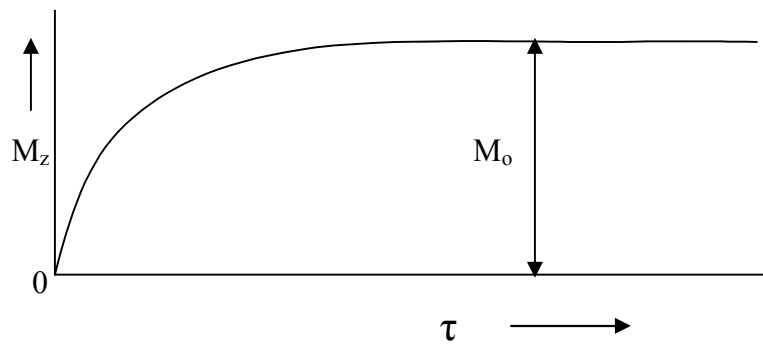
If the tip angle of the magnetization M_z is θ , the expression for the steady state

magnetization is

$$M_z = M_o \frac{(1 - e^{-\frac{\tau}{T_1}}) \sin \theta}{(1 - \cos \theta \times e^{-\frac{\tau}{T_1}})} \quad (1.74)$$



(a)



(b)

Figure 1.8 (a) The Saturation burst pulse sequence (b) the growth of magnetization.

This means that the magnetization recovery shape is a unique function of the tip angle so that both θ and T_1 can be obtained from the same experiment. Note that the range in which M_z changes is reduced to half. This pulse sequence is ideal whenever T_1 is greater than 1 sec and long waiting time between any two T_1 measurements is drastically reduced.

References

1. Sakurai. *Modern Quantum Mechanics* (Addison- Wesley Publishing Company Inc., Massachusetts, **1994**).
2. Slichter CP. *Principles of Magnetic Resonance* (Springer-Verlag, Berlin Heidelberg, New York, **1978**).
3. Abragam A. *The Principles of Nuclear Magnetism* (Oxford University Press, Oxford, UK, **1961**).
4. Andrew ER. *Nuclear Magnetic Resonance* (University Press, Cambridge, UK, **1958**).
5. Pake GE. *J. Chem. Phys.*, **16(4)**, 327, (1948).
6. Andrew ER and Bersohn R. *J. Chem. Phys.*, **18(2)**, 159, (1950).
7. Gutowsky HS, Pake GE and Bersohn R.. *J. Chem. Phys.*, **22(4)**, 643, (1954).
8. Bersohn R., and Gutowsky HS. *J. Chem. Phys.*, **22(4)**, 651, (1954).
9. Itoh J, Kusaka R, Yamagata Y, Kiriyama R and Ibamoto H. *J. Phy. Soc. Jpn.*, **8**,
10. 293 (1953).
11. Itoh J, Kusaka R and Saito Y. *J. Phy. Soc. Jpn.*, **17**, 463 (1962).
12. Lalowicz ZT, McDowell CA and Raghunathan P. *J. Chem. Phys.*, **70(11)**, 4819, (1979).
13. Van Vleck JH. *Phys. Rev.*, **74(9)**, 1168 (1948).
14. Andrew ER and Eades RG. *Proc. Roy. Soc.*, **A 218**,537 (1953).
15. Bloembergen N, Purcell EM and Pound PN. *Phys. Rev.*, **73(7)** 679 (1948).
16. Torrey HC. *Phys. Rev.*, **92(4)**, 962 (1953).
17. Hubbard PS. *Phys. Rev.*, **131(3)**, 1155 (1963).
18. Sitnitsky AE, Pimenov GG and Anisimov AV. *J. Mag. Reson.*, **172**, 48 (2005).
19. Allen PS and Cowking A. *J. Chem. Phys.*, **47(11)**, 4286 (1967).
20. Allen PS and Clough S. *Phys. Rev. Lett.*, **22(25)**, 1351 (1969).
21. Koksai F, Rossler E and Sillescu H. *J. Phys. C: Solid State Phys.*, **15**, 5821(1982).
22. Wallach D and Steele WA. *J. Chem. Phys.*, **52**, 2534, (1970).
23. Allen PS and Howard CJ. *Mag. Res and Rel Phen, Colloq AMPERE*, 637 (1970).
24. Horsewill Progr. In Nucl. *Mag. Reson. Spectro.*, **35**, 359 (1999).

25. Svare I and Tunstall DP. *J. Phys. C: Solid State Phys.*, **8**, L559 (1975).
26. Hund F. *Z. Phys.*, **43**, 805 (1927).
27. Svare I, Raaen AM and Fimland BO, *Physica B*, **128B** 144 (1985).
28. Svare I, Raaen AM and Thorkildsen G. *J. Phys. C: Solid State Phys.*, **11**, 4069 (1978).
29. Ylinen EE, Tuohi JE and Niemela LKE, *Chem. Phys. Lett.*, **24(3)**, 447 (1974).
30. Clough S, Horsewill AJ, Johnson MR, Sutchcliffe JH, and Tomsah IBT. *Mol. Phys.*, **81**, 975 (1994).
31. Ingman LP, Punkkinen M, Vuorimaki AH and Ylinen EE. *J. Phys. C: Solid State Phys.*, **18**, 5033 (1985).
32. Tuohi JE, Ylinen EE and Punkkinen M. *Phys. Scr.*, **13**, 253 (1976).
33. Ingman LP, Punkkinen M, Ylinen EE, and Dimitropoulos C. *Chem. Phys. Lett.*, **125(2)**, 170 (1986).
34. Lalowicz ZT, Werner U and Muller Warmuth. *Z. Naturforsch*, **43a**, 219,895 (1989).
35. Cavagent. D., Tevino SF and Magerl A. *J. Phys: Condens Matter*, **1**, 10047 (1989).
36. Ingman LP, Koivula E, Lalowicz ZT, Punkkinen M and Ylinen EE. *Z. Phys. B – Condens. Matter*, **81**,175 (1990).
37. Heuer A. *Z. Phys. B – Condens. Matter*, **88**, 39 (1992).
38. Latanowicz L and Medycki. *J. Phys. Chem. A*, **111(7)**, 1351(2007).
39. Horsewill AJ, Alsanoosi AM and Carlile. CJ. *J. Phys. C: Solid State Phys.*, **20**, L869 (1987).
40. Haupt J. *Z. Naturforsch*, **26a**, 1578 (1971).
41. Punkkinen M. *J. Mag. Reson.*, **19**, 222 (1975).
42. Clough S and McDonald P J. *J. Phys. C: Solid State Phys.*, **15**, L1039 (1982).
43. Sobol WT, Sridharan K R, Camerib. IG and. Pintar MM. *Z. Naturforsch*, **40a**, 1075 (1985).
44. Sridharan K R, Sobol WT and. Pintar MM. *J. Chem. Phys.*, **82(11)**, 4886 (1985).
45. Ligthelm DJ, Wind RA and Smidt J. *Physica B*, **100B**, 175 (1980).
46. Fukushima E and Roeder SBW. *Experimental pulse NMR: A nuts and bolts approach* (Addison- Wesley Publishing Company Inc., Massachusetts, 1981).